Photoinduced Electron Transfer Reactions by SmI_2 in THF: Luminescence Quenching Studies and Mechanistic Investigations

Edamana Prasad,[a] Brian W. Knettle,[b] and Robert A. Flowers II*[a]

Abstract: Photoluminescence quenching studies of SmI_2 in dry THF were carried out in the presence of five different classes of compounds: ketone, alkyl chloride, nitrile, alkene and imine. The free energy change (ΔG^0) of the photoinduced electron transfer (PET) reactions was calculated from the redox potentials of the donor (SmI_2) and acceptors. The bimolecular quenching constants (k_q) derived from the Stern–Volmer experiments parallel the free energy changes of the PET processes. The observed quenching constants were compared with the theoretically derived electron transfer rate constants (k_{et}) from Marcus theory and found to be in good agreement when a value of $\lambda = 167\ \mathrm{kJ\,mol^{-1}}$ ($40\ \mathrm{kcal\,mol^{-1}}$) was used for the reorganization energy of the system. A careful comparison of the excited state dynamics of Sm^{II} in the solid state to the results obtained in solution (THF) provides new insight in to the excited states of Sm^{II} in THF. The activation parameters determined for the PET reactions in SmI_2/1-chlorobutane system are consistent with a less ordered transition state and high degree of bond reorganization in the activated complex compared to similar ground state reactions. Irradiation studies clearly show that SmI_2 acts as a better reductant in the excited state and provides an alternative pathway for rate enhancement in known and novel functional group reductions.

Keywords: Marcus theory · photochemistry · samarium · solution photodynamics

Introduction

Applications of SmI_2 to organic chemistry have been significantly advanced since its first discovery by Kagan and coworkers in 1980.[1] Since then, this reagent has become a useful and essential component in the reduction and reductive coupling of many organic functional groups.[2] In particular, the reduction of ketones to alcohols and the reductive coupling of carbonyl compounds with olefins provides a wide range of strategies for the synthesis of natural products including (±)-muscone, upial, paeoniflorigenin, (−)-grayanotoxin and (−)-steganone.[3] Another notable feature of SmI_2-mediated reductions is the high degree of diastereoselectivity further extending its utility in organic synthesis.[4]

A number of SmI_2-based reactions such as the reduction of dialkyl ketones, imines, and bromoalkanes by SmI_2 are slow and the presence of additives such as hexamethylphosphoramide (HMPA), transition metal catalysts and inorganic acids or bases is necessary for successful reaction outcomes.[5] The most utilized additive in reactions of SmI_2 is HMPA since it not only enhances the rate but also the diastereoselectivity of many reactions.[2,5a,6] Other basic cosolvents capable of acting as ligands have been utilized in reactions of SmI_2 and these include 1,3-dimethyl-3,4,5,6-tetrahydro-2(1*H*)-pyrimidinone (DMPU)[7a] and nitrogen donor solvents.[7b] Although all of these additives have found applications in a number of reactions, none provide the general utility of HMPA. Since HMPA is a suspected human carcinogen, its utilization should be limited whenever possible.

Alternative means of enhancing the rate of Sm^{II}-mediated reduction reactions is of paramount importance and several protocols have been suggested to attain this target.[8,9] Photo-excitation of Sm^{II} complex is one among them. In 1997, Ogawa et al. reported that upon irradiation with visible light, SmI_2 was able to reduce chloroalkanes.[9] In a different study, Molander and co-workers described a number of sequential reactions and intramolecular ketone–nitrile reductive coupling reactions promoted by photo-excited samarium(II) iodide.[10] Although there are several studies de-

---

[a] Dr. E. Prasad, Prof. R. A. Flowers II
Department of Chemistry, Lehigh University
Bethlehem PA 18015 (USA)
Fax: (+1) 610-758-6536
E-mail: rof2@lehigh.edu

[b] Dr. B. W. Knettle
Department of Natural Sciences
University of Virginia's College at Wise
Science Center 109, 1 College Avenue Wise VA 24293 (USA)

Supporting information for this article is available on the WWW under http://www.chemeurj.org/ or from the author.

DOI: 10.1002/chem.200401163

scribing the mechanistic pathways of SmI_2 and SmI_2/HMPA reduction of substrates, there exist very few studies about the mechanistic investigations of excited SmI_2 chemistry in solution. A relatively recent laser flash photolysis study by Skene et al. revealed that SmI_2 in THF reduced alkyl and aryl halides through electron transfer from the excited SmI_2.[11] While these elegant studies dealt with the enhanced reactivity of excited SmI_2, they did not describe the excited state dynamics of SmI_2. The few previous studies which deal with the excited state Sm^{II} species described the solid state chemistry of Sm^{II} embedded in inorganic crystal lattices.[12] The aim of the present study is to understand the mechanistic details of the excited SmI_2 in THF and utilize this knowledge to carry out novel organic reactions mediated by SmI_2. Luminescence quenching studies of SmI_2 in THF have been carried out in the presence of a ketone, alkyl chloride, nitrile, alkene and an aryl imine. The quencher concentrations were minimized to avoid any type of ground state interaction between Sm and substrates. The bimolecular quenching constants obtained from these studies were compared with the theoretical values of electron transfer rate constants. The dynamics of the excited state reactions of SmI_2 in THF are discussed based on comparison of the solid state chemistry of Sm^{II} to the results obtained in solution.

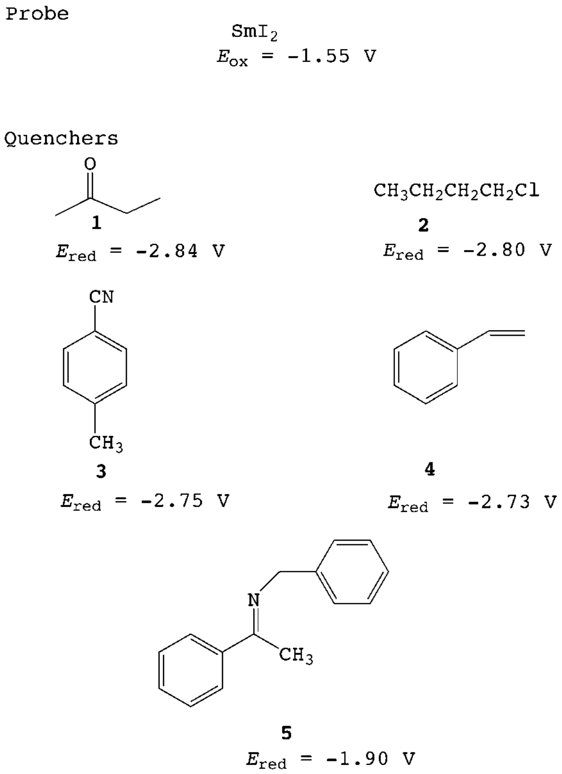

Figure 1. Probe, quenchers, and their redox potentials used in this study. The redox potentials are all referenced to SCE.

Results and Discussion

In the present study, the probe molecule was SmI_2 and quenchers were 2-butanone, 1-chlorobutane, 4-tolunitrile, styrene and the benzyl-(1-phenyl-ethylidene)-amine (Figure 1). These quenchers were selected for three reasons: a) First, they do not react with SmI_2 in the ground state. Reduction of 1-chlorobutane, styrene, 4-tolunitrile and the benzyl-(1-phenyl-ethylidene)-amine by SmI_2 in the ground state does not occur and reduction of 2-butanone is very slow ($7 \pm 3 \times 10^{-4}\,\text{M}^{-1}\text{s}^{-1}$).[13] b) Second, none of these quenchers except 2-butanone are expected to complex with SmI_2 in the ground state. For 2-butanone, the concentration of the quencher was kept below the point where the Stern–Volmer plot deviates from linearity to avoid any complex formation with the probe. c) Finally, these quenchers are known to be reduced by the SmI_2/HMPA combination through an electron transfer mechanism.[14] The UV/Vis spectra of SmI_2 in presence of these quenchers were examined at the experimental concentrations and the spectra appear as the superposition of the spectra of the individual components indicating that charge transfer formation and static quenching is avoided under our experimental conditions.

The absorption spectrum of SmI_2 in THF at 25 °C is shown in Figure 2. In the solid state, these absorption bands are attributed to transitions from the $4f^6$ state ($^7F_0$) of the metal to the $4f^5 5d^1$ states.[15–18] Yanase has developed an approximate, analytical description of the energy levels for the $4f^5 5d^1$ configuration of the Sm^{II} in the SrF_2 crystals.[15] The $5d^1$ electron experiences a large crystal field splitting compared with the 4f electrons, which results in splitting the 5d orbital into e_g and t_{2g} components. The elegant study of Payne et al. shows that the two lowest energy levels (^6H and ^6F) arising from $4f^5$ metal core, couple to the e_g and t_{2g} orbital components of the $5d^1$ electron to form four discrete energy levels, described by term symbols as $^6H_{eg}$, $^6F_{eg}$, $^6H_{t2g}$ and $^6F_{t2g}$.[16] The main absorption peaks observed in the solid-state UV/Vis spectra of SmI_2 were attributed to the electronic transitions to these four different fd excited states. The energy for these transitions calculated from their reported wavelengths are $16.5 \times 10^3\,\text{cm}^{-1}$ (590 nm), $24 \times 10^3\,\text{cm}^{-1}$ (417 nm), $31 \times 10^3\,\text{cm}^{-1}$ (322 nm), and $40 \times 10^3\,\text{cm}^{-1}$ (250 nm) for $^6H_{eg}$, $^6F_{eg}$, $^6H_{t2g}$ and $^6F_{t2g}$, respectively.[16] Comparison of the UV spectrum of SmI_2 in THF shows a close similarity in the transition energies (except that, the peaks at low energy region appear as two broad bands) implying *identical* electronic transitions in both solid SrF_2 crystals and in THF.

The spin of the $5d^1$ electron can be oriented either parallel or antiparallel to the total spin of the $4f^5$ state and is controlled by the exchange interaction between the d and f states. For Sm^{II}, excited state 5d electron prefers to be in the opposite spin state due to the exchange interaction.[17] Upon photoexcitation, the electron in Sm^{II} is excited to the fd states of the same multiplicity (an allowed transition) and relaxed to the lowest excited state through a spin inversion. Emission of the electron takes place from this lowest 4f

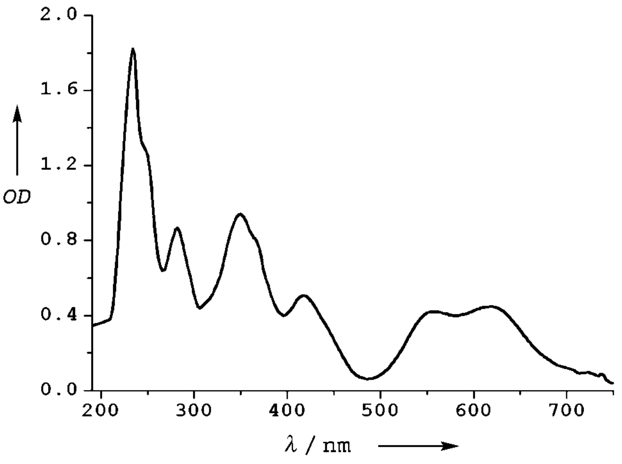

Figure 2. Absorption spectrum of SmI_2 (2.5 mM) in THF.

electronic state, designated as $^5D_0$, to the ground state, which is $^7F_0$. Extensive studies on the solid-state chemistry of Sm^{II} by Payne,[16] Dorenbos,[17] McClure and Kiss,[18] have revealed that the emission process in Sm^{II} is in-between the $^5D_0$ and $^7F_0$ levels. While these studies were carried out in the solid state, care should be taken to compare these results to the solution phase. To account for the role of solvent dynamics in THF, the first excited state energy (E_{00}) of Sm^{II} was determined in THF and compared with the reported value in solid state. The value, E_{00}, was calculated from the point of intersection of the absorption and emission spectra in THF (Figure 3). The value obtained was 14516 cm^{-1}, which closely matches the energy of $^5D_0$–$^7F_0$ emission line obtained by Payne et al. (14616 cm^{-1}).[16] This leaves us with the following two possibilities: a) The emission process in Sm^{II} involves the same energy levels (^5D to ^7F) in both the solid state and in THF solution or b) the emission process in SmI_2 in THF is from the lowest fd state, which is placed near to the $^5D_0$ state due to THF solvation.

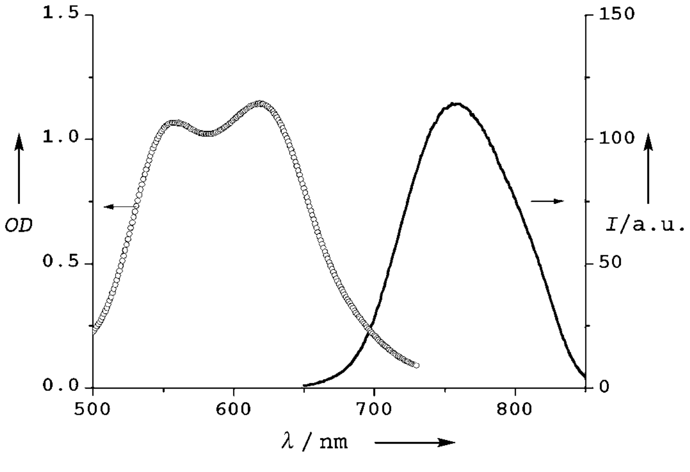

Figure 3. Absorption spectrum and emission spectrum of SmI_2 (2.5 mM) in THF. The wavelength at absorption and emission spectra overlap is 697 nm.

Luminescence lifetime study is one of the best ways to characterize the excited states of a species in solution. The reported value for the lifetime of SmI_2 in THF at room temperature is 125 ns.[11] After carefully removing all the impurities in THF by using an Innovative Technologies solvent purification system and carefully degassing it, an increase in the lifetime of SmI_2 in THF to 240 ± 10 ns at 25 °C was observed. A careful literature survey was carried out to compare the lifetime values for the strongest emission line of Sm^{II} in the solid state. In CaF_2 crystal the value is 2×10^{-6} s at 77 K and a much longer lifetime value (2×10^{-2} s) was found in SrF_2 at 20 K; this suggests that temperature also has a tremendous effect on the lifetime of Sm^{II}.[12b] The reported values imply that the emission from the excited state of Sm^{II} is a slow process and more likely to be a result of the intersystem crossing of the excited electron upon emission. The longer lifetime observed in solution is presumably either due to the thermal population of the closely spaced fd states ($4f^55d^1$) from the lowest excited state ($^5D_0$) at room temperature, or to a "heavy atom effect", caused by the presence of iodine in SmI_2. The thermal population of the fd states at room temperature makes the emission a quantum mechanically allowed transition.[19] On the other hand, a heavy atom effect due to the presence of iodine facilitates the spin inversion of the electron resulting faster intersystem crossing.[20]

It is interesting to note that there are striking similarities between the results obtained from the spectroscopic investigation of Sm^{II} embedded in a crystal lattice (SrF_2) and SmI_2 in THF. The Sm^{II} ion in the SrF_2 crystal is surrounded by a cube of F^- ions.[18] The crystal structure published by Evans and co-workers showed that SmI_2 crystallized from THF is surrounded by five THF molecules and two iodine atoms.[21] Since the absorption process involves an electronic transition from the f to the d orbitals of the metal, it is reasonable to assume that the ligands around Sm could interact with the much spatially oriented d orbital, resulting in similar perturbations of the excited fd states. Also, the emission spectra in the solid state and in THF exhibit similar features. It is worth mentioning here that Sm^{II} in $SrCl_2$ gives a broad emission spectrum at room temperature (the onset of the emission is 650 nm and ends at 770 nm) very similar to that obtained in THF.[12c] If the emission process in SmI_2 involves only f orbitals (between $^5D_0$ and $^7F_0$), why should it be a broad emission spectrum rather than a line spectrum? Investigation of the solid-state chemistry of Sm^{II} embedded in crystal lattices of SrF_2 and $SrCl_2$ show that at very low temperature(4.2 K),[12b] the emission loses the broad feature and consists of individual lines. This implies that at elevated temperature, the fd states are thermally populated and the emission process involves 4f5d to 4f transition, which explains both the broadness of the spectrum and the increased radiative lifetime. To test this hypothesis, a pilot experiment was carried out in which the decay of the excited SmI_2 in THF was compared at two different temperatures (see Figure S12 in the Supporting Information). The results indicate that the excited state lifetime of SmI_2 increased considerably when the temperature was reduced from 25 to 0 °C suggesting that thermal population of fd states plays a role in the excited state lifetime of SmI_2 in THF. Based on the scenarios described above, the excited state dynamics of SmI_2 in THF are summarized in Figure 4.

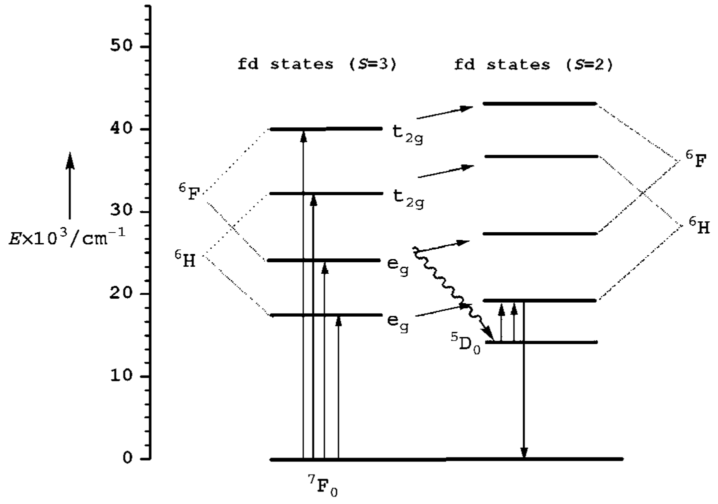

Figure 4. Schematic representation of excited state dynamics of SmI_2 in THF. Excitation of a single electron from ^7F state provides the excited fd states with $S=3$. The ^6H and ^6F states arising from the $4f^5$ core couple to the e_g and t_{2g} orbital components of the 5d electron to form the four states drawn in the left side of the scheme. The exchange interaction flips the spin of the excited electron and results in an intersystem crossing to the $^5D_0$ state. The fd states with $S=2$ are thermally populated at room temperature from which the emission takes place to the ground state. In solution, the lowest fd state with $S=2$ is placed near to $^5D_0$ levels (not shown in the scheme) due to the solvation effect of THF. The energy levels are assumed to be similar to that in solid state Sm^{II}.

The excitation spectrum of SmI_2 was taken in THF at different concentrations and is shown in Figure 5. The luminescence intensities were collected at 760 nm and the excitation scan was run from 200 to 750 nm. The excitation spectrum of SmI_2 in THF resembles the absorption spectrum closely except that the intensity of the peaks is altered, resulting in more intense peaks in the visible region. This suggests that the excited electron has efficiently undergone intersystem crossing only when excited in the visible wavelength. At higher concentrations of SmI_2, the intensity of UV bands in the excitation spectrum is further reduced (see Supporting Information). The comparatively high extinction coefficient of the UV peaks of SmI_2 to that in the visible region may lead to a self-quenching of the excited state on blue wavelength excitation at the experimental concentrations (for example, molar extinction coefficients for SmI_2 peaks at 351 and 618 nm are 1323 ± 3 and 584 ± 22 $mol^{-1}cm^{-1}$, respectively).[22] Regardless of the complexities of the intersystem crossing process, this experimental result explains the observation by Ogawa et al. that efficient photoreaction by SmI_2 occurred only when excited at $>$ 500 nm.[9a]

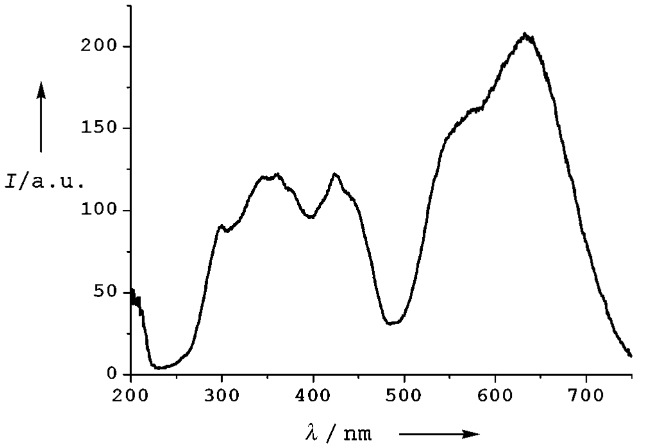

Figure 5. Excitation spectrum of SmI_2 (2.5 mM) in THF. The luminescence intensity was collected at 760 nm and the excitation scan was run from 200 to 750 nm.

The SmI_2 luminescence appears as a broad band between 650 and 850 nm with a maximum at 760 nm. The bimolecular quenching constant for each system was obtained from the Stern–Volmer Equation (1).

$$\frac{I_0}{I} = 1 + K_{sv}\,[Q] \tag{1}$$

where I_0 and I are the intensities of the SmI_2 luminescence in the presence and absence of quencher, respectively, K_{sv} is the Stern–Volmer constant and [Q] is the quencher concentration. The natural lifetime, τ_0, of SmI_2 in THF was determined to be 240 ± 10 ns. The bimolecular quenching constant (k_q) for different systems was then calculated by using Equation (2).

$$k_q = \frac{K_{sv}}{\tau_0} \tag{2}$$

Figure 6 shows the luminescence quenching spectra of SmI_2 by the 1-chlorobutane in THF at 25 °C. The corresponding Stern–Volmer plot is shown in Figure 7. The bimolecular quenching constants obtained from the experiment are given in Table 1.

Next, the reduction potential of the quenchers was determined in DMF versus the $Ag/AgNO_3$ reference electrode. The reduction potential could not be determined in THF since the values are outside the potential window of this solvent. The E_{red} values are shown in Figure 1. The free energy for the electron transfer in THF was calculated by using Equation (3), where E_{00} is the first excited state energy of Sm^{II}, E_{ox} is the oxidation potential of the donor, E_{red} is the reduction potential of the acceptor, ε is the dielectric constant of THF, r_P and r_Q are the radii for the probe and quencher molecules, respectively, and d is the distance separating the probe and quencher.[23]

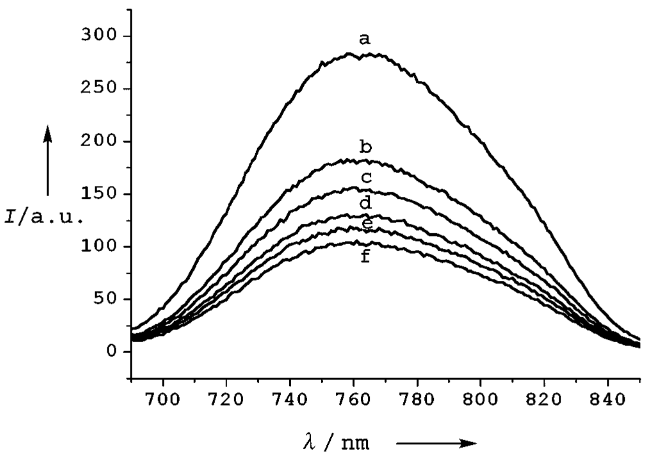

Figure 6. Luminescence quenching of SmI_2 (5 mM) in presence of 1-chlorobutane in THF. The concentrations of 1-chlorobutane are a) 0 M, b) 0.02 M, c) 0.04 M, d) 0.06 M, e) 0.08 M, and f) 0.10 M. The excitation wavelength was 500 nm.

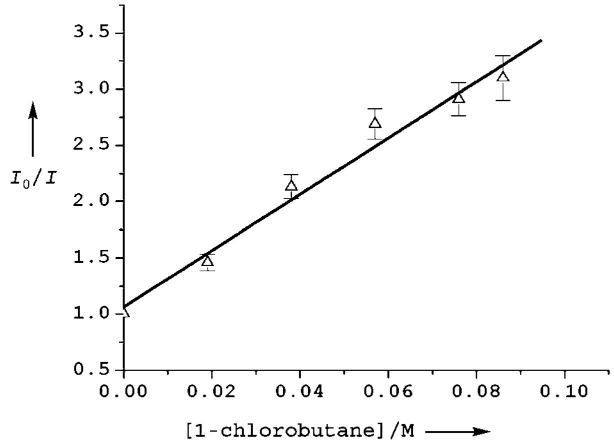

Figure 7. Stern–Volmer plot obtained from the luminescence quenching studies of SmI_2/1-chlorobutane system.

$$\Delta G^0 = E_{\rm ox} - E_{\rm red} - E_{00} - \frac{e^2}{2}\left(\frac{1}{r_{\rm P}}+\frac{1}{r_{\rm Q}}\right)\left(\frac{1}{37}+\frac{1}{\varepsilon}\right) - \frac{e^2}{\varepsilon d} \quad (3)$$

The value of r_P was taken as 5.6 Å.[24] The values of r_Q were taken from the molecular model of each quencher by using Spartan Essential software. The separation distance d was taken as the sum of the radii of the donor and acceptor. The redox potentials of the probe and the quenchers are given in Figure 1 and the calculated ΔG^0 values are presented in Table 1. The thermodynamic redox potentials of the imine and styrene were evaluated by using the approach described by Parker.[25] The redox potentials of the other substrates were obtained from literature sources.[26] We are aware that neglect of kinetic shifts of peak potentials (in the case of the redox potentials obtained from literature sources) can lead to errors in derived thermochemical quantities. The fact that the experimental quenching constants (k_q) for reduction of substrates parallel their redox potentials suggests that the redox potentials are thermodynamically significant. Furthermore, inspection of the values in Table 1 shows that the luminescence quenching rate constants parallel the free energy change of the PET reaction.

Table 1. Free energy change, bimolecular quenching constants (k_q) and theoretically derived electron transfer rate constants (k_{et}) in SmI_2 mediated PET reactions ($\lambda = 167$ kJ mol^{-1}). The calculated values for k_{et} with $\lambda = 293$ kJ mol^{-1} are shown in parentheses.

Quencher	ΔG^0 [kJ mol^{-1}]	k_q [M^{-1}s^{-1}]	k_{et} [M^{-1}s^{-1}]
2-butanone	−65.7	$2.0 \pm 0.1 \times 10^7$	1.4×10^8 (1.3×10^3)
1-chlorobutane	−71.5	$1.0 \pm 0.1 \times 10^8$	2.7×10^8 (3.3×10^3)
4-tolunitrile	−78.7	$13.0 \pm 0.2 \times 10^8$	6.0×10^8 (9.5×10^3)
styrene	−80.8	$1.2 \pm 0.1 \times 10^8$	7.1×10^8 (1.3×10^4)
benzyl(1-phenylethylidene)amine	−105.0	$2 \pm 1 \times 10^9$	4.5×10^9 (3.7×10^5)

According to Marcus theory, the electron transfer rate constant between a donor and an acceptor is given by Equation (4)[27]

$$k_{\rm et} = \frac{k_{\rm d}}{[1 + 0.25\exp\{(\lambda + \Delta G^0)^2/4\lambda RT\}]} \quad (4)$$

where k_d is the diffusion controlled rate constant, λ is the reorganization energy and ΔG^0 is the free energy change of the PET reaction. The diffusion controlled rate constant in THF was determined by the Stokes–Einstein–Smoluchowski equation and the value was found to be 1.4×10^{10} M^{-1}s^{-1}.[28]

Reorganization energy is the sum of the energies required to reorganize the molecular structure of the reactants (λ_{is} = inner sphere contribution) and the surrounding solvent molecules (λ_{os} = outer sphere contribution) to the configuration compatible with electron transfer and was estimated to be approximately 167 kJ mol^{-1} from a fit to the Marcus equation and the experimental data. While different structural features of the quenchers are expected to have an effect on λ_{is}, we reasoned taking a single value of λ for the entire donor–acceptor series by the fact that in moderately polar solvents λ_{os} will have a predominant contribution towards total reorganization energy.[29]

The elegant work of Daasbjerg and co-workers provides a value ~293 kJ mol^{-1} for self-exchange reorganization energy of Sm^{3+}/Sm^{2+} system in THF.[30] Since the self-reorganization energies of alkyl chlorides fall in the range of 234–377 kJ mol^{-1}[31] one would expect an average value for the total reorganization energy of the system to be closer to 293 kJ mol^{-1}. When a value of 293 kJ mol^{-1} for total λ for the present system is used, the fit deviated substantially from the experimental points (Figure 8).

This can be interpreted in one of two ways: 1) The λ value is approximately 167 kJ mol^{-1} and photoexcited SmI_2 is initiating electron transfer through a predominantly outer-sphere pathway, or 2) the λ value is higher (closer to 293 kJ mol^{-1}) and the experimental rate constants are larger than predicted by Marcus theory, suggesting that photoexcited SmI_2 initiates electron transfer through a pathway containing a higher degree of inner-sphere ET.

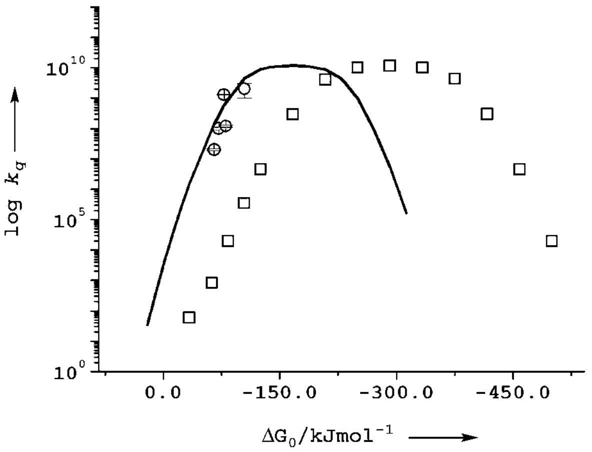

Figure 8. Comparison of experimental data with the Marcus curve by using two different λ values. The solid line is for $\lambda = 167$ kJ mol^{-1} and the squares are for $\lambda = 293$ kJ mol^{-1}. The experimental points are shown as circles.

Inner-sphere ET is characterized by a substantial degree of bonding interaction between donor–acceptor pairs along the reaction coordinate that is, in the ground state or approaching the transition state. Spectroscopic experiments have shown that under the conditions of the experiments reported herein, the presence of a large excess of substrate shows no perturbation of the UV/Vis spectrum of SmI_2 in THF. While this finding is consistent with little interaction between SmI_2 and substrates in the ground state, Stern–Volmer experiments show that only collisional quenching is occurring in these experiments as well. Static quenching (through coordination between SmI_2 and substrates) is evident when the Stern–Volmer plots deviate from linearity. Under the conditions of these experiments, this deviation was not observed. The classic work of Eberson shows that the λ values for a wide variety of single electron transfer reagents in their reactions with a range of alkyl halides are in the 167–209 kJ mol^{-1} range.[31] Furthermore, earlier work of Moore suggests that the presence of large polarizable ligands on metals (such as I^-) results in lower λ values for metal complexes.[32] Based on this analysis, a λ value of approximately 167 kJ mol^{-1} best represents the system under study in this report. The theoretical values obtained are presented in Table 1.

Regardless of the discrete mechanistic details of ET from photoexcited SmI_2, the data clearly show that light induced electron transfer provides an alternative pathway for rate enhancement of SmI_2 mediated reduction reactions for a wide variety of substrates. Furthermore, these results show that even olefins can be reduced. To verify the photochemical initiated olefin reduction, the reaction of SmI_2 and styrene was examined on a preparative scale. A tungsten halogen lamp (100 W) placed at 100 cm away from the reaction mixture was used as the light source. Irradiation of a solution of styrene in THF in the presence of four equivalents of SmI_2 for a *few minutes* resulted in the formation of ethylbenzene. A blank experiment was performed in which styrene was mixed with four equivalents of SmI_2 in THF and kept for 10 h without irradiation to give the starting material intact. This clearly shows the high reactivity of photo-excited SmI_2.

To obtain a better understanding of the underlying parameters that control the photoinduced electron transfer reactions of SmI_2, a temperature dependent study of the luminescence quenching of SmI_2 in the presence of 1-chlorobutane was initiated as a representative sample. The quencher concentration was varied in a Stern–Volmer fashion and the steady-state luminescence quenching constants for SmI_2/1-chlorobutane system were measured over a range of temperature from 5 to 45 °C. The activation parameters obtained from the temperature dependent study are shown in Table 2. The Eyring plot for the system is shown in Figure 9.

Table 2. Activation parameters obtained from the temperature dependent luminescence quenching studies of SmI_2/1-chlorobutane system in THF.

System	$\Delta S^{\neq[a]}$ [J mol^{-1} K^{-1}]	$\Delta H^{\neq[a]}$ [kJ mol^{-1}]	$\Delta G^{\neq[b]}$ [kJ mol^{-1}]
SmI_2/1-chlorobutane	-29 ± 4	19.3 ± 0.4	27.6 ± 0.4

[a] Eyring activation parameters were obtained from $\ln(k_{obs}h/kT) = -\Delta H^{\neq}/RT + \Delta S^{\neq}/R$. [b] Calculated from $\Delta G^{\neq} = \Delta H^{\neq} - T\Delta S^{\neq}$.

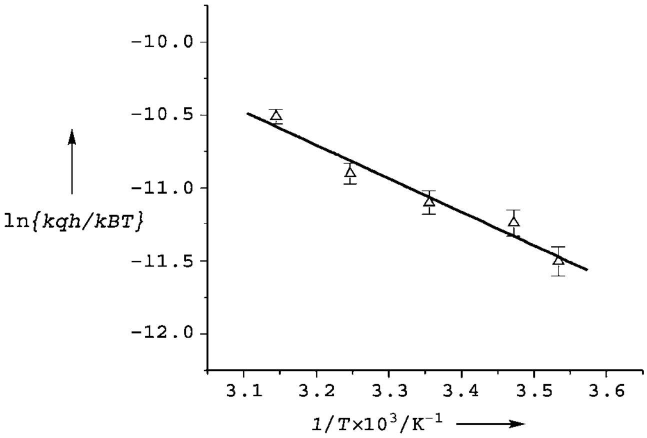

Figure 9. Eyring plot obtained from the luminescence quenching studies of SmI_2/1-chlorobutane system.

Inspection of the values in Table 2 indicates that the activation of enthalpy of the PET reaction is very low suggesting considerable bond reorganization between the metal and the substrate in the transition state. The free energy of activation is consistent with a fast electron transfer step. A less negative value of the entropy is not uncommon in many PET reactions; especially in biradical PET reactions.[33] In general PET reactions involve more polarized transition states leading to large solvent reorganization, before and after the electron transfer, making the transition state less ordered than ground state reactions. These PET reactions are less temperature sensitive, suggesting that reaction is enthalpically rather than entropically driven.

Conclusion

Photoluminescence quenching experiments of SmI_2 conducted in dry THF with 2-butanone, 1-chlorobutane, styrene, 4-tolunitrile and benzyl-(1-phenyl-ethylidene)-amine clearly show that SmI_2 acts as a better reductant in the excited state and provides an alternative pathway for rate enhancement in SmI_2-mediated reduction reactions, a finding in agreement with previous studies. In fact, photoirradiation of SmI_2 in THF reduced styrene to ethylbenzene, while ground state SmI_2 failed to react at all. Clearly, photoexcited SmI_2 is highly reactive and presumably can accelerate or promote reactions not accessible by the combination of SmI_2-HMPA. The observed quenching constants were in good agreement with the theoretically derived electron transfer rate constants (k_{et}) from Marcus theory when a λ value of 167 kJ mol^{-1} was used. Further study of the excited state dynamics of SmI_2 and other Sm^{II}-based reductants using transient absorption techniques, lifetime studies and the exploration of novel photoinduced reactions are currently under investigation in our laboratory.

Experimental Section

Methods: UV/Vis experiments were performed on a Shimadzu UV-1601 UV-Visible Spectrophotometer controlled by UV Probe (version 1.11) software. Cyclic voltammetry experiments were performed on a BAS 100B/W MF-9063 Electrochemical Workstation. Solutions of quenchers ($1\times10^{-3}\,\text{M}$) in DMF containing 0.1 M tetrabutylammonium hexafluorophosphate as supporting electrolyte were thoroughly degassed before use. A glassy carbon electrode was used as the working electrode and a platinum wire was used as the counter electrode. The reduction potential values for 2-butanone, 1-chlorobutane, and 4-tolunitrile were taken from literature.[26] Luminescence experiments were performed on a Photon Technology International fluorimeter utilizing a XenoFlash power supply and MD-5020 motor driver. This equipment was controlled by the FeliX32 Analysis Version 1.0 (build 44) software package. Temperature dependent luminescence quenching studies were carried out using a Varian Cary Eclipse model Fluorescence spectrophotometer. Luminescence lifetime studies were carried out by exciting the sample in THF by a Nd/YAG nanosecond laser at 480 nm. Spartan Essential software (version 1,0,2) by Wavefunction was utilized for the determination of molecular diameters of reagents involved in dynamic quenching experiments. For the luminescence studies, the concentrations of SmI_2 were kept as 5 mM and quencher concentrations were in the average range of 10–50 mM.

Material and general procedures: THF was distilled from sodium/benzophenone, under nitrogen atmosphere. Dried solvents were stored in an Innovative Technology drybox containing a nitrogen atmosphere and a platinum catalyst for drying. The SmI_2 was prepared according to a reported procedure.[34] The concentration of the SmI_2 was determined by iodometric titration.[35] 2-Butanone, 1-chlorobutane, styrene and 4-tolunitrile were purchased from Aldrich and distilled before use. Benzyl-(1-phenylethylidene)amine was synthesized according to a reported procedure.[36]

Acknowledgements

R.A.F. is grateful to the National Science Foundation (CHE-0413845) for support of this work. We thank Professor Ivan Biaggio of the Department of Physics at Lehigh University for use of the Nd/YAG laser utilized in the luminescence lifetime studies, Drs. K. R. Gopidas (Photosciences and Photonics Division, Regional Research Laboratory (CSIR), Trivandrum, India), Kamil Klier, and Rebecca S. Miller (Department of Chemistry, Lehigh University) for their useful comments on the manuscript. We also thank referees 1 and 2 for their insightful comments on the manuscript.

---

[1] P. Girard, J. L. Namy, H. B. Kagan, *J. Am. Chem. Soc.* **1980**, *102*, 2693–2698.
[2] G. A. Molander, C. R. Harris, *Chem. Rev.* **1996**, *96*, 307–338.
[3] a) H. Suginome, S. Yamada, *Tetrahedron Lett.* **1987**, *28*, 3963–3966; b) H. Nagaoka, K. Shibuya, Y. Yamada, *Tetrahedron Lett.* **1993**, *34*, 1501–1504; c) E. J. Corey, Y.-J. Wu, *J. Am. Chem. Soc.* **1993**, *115*, 8871–8872; d) T. Kan, S. Hosokawa, S. Nara, M. Oikawa, S. Ito, F. Matsuda, H. Shirahama, *J. Org. Chem.* **1994**, *59*, 5532–5534.
[4] G. A. Molander, *Chem. Rev.* **1992**, *92*, 29–68.
[5] a) J. Inanaga, M. Ishikawa, M. Yamaguchi, *Chem. Lett.* **1987**, 1485–1486; b) J. Inanaga, Y. Yokoyama, Y. Baba, M. Yamaguchi, *Tetrahedron Lett.* **1991**, *32*, 5559–5562; c) Y. Kamochi, T. Kudo, *Tetrahedron* **1992**, *48*, 4301–4312; d) Y. Kamochi, T. Kudo, *Tetrahedron Lett.* **1991**, *32*, 3511–3514.
[6] G. A. Molander, J. A. McKie, *J. Org. Chem.* **1992**, *57*, 3132–3139.
[7] a) E. Haesegawa, D. P. Curran, *J. Org. Chem.* **1993**, *58*, 5008–5010; b) W. Cabri, I. Candiani, M. Colombo, L. Franzoi, A. Bedeschi, *Tetrahedron Lett.* **1995**, *36*, 949–952.
[8] a) A. Dahlen, G. Hilmersson, B. W. Knettle, R. A. Flowers II, *J. Org. Chem.* **2003**, *68*, 4870–4875; b) E. Prasad, B. W. Knettle, R. A. Flowers II, *J. Am. Chem. Soc.* **2004**, *126*, 6891–6894.
[9] a) A. Ogawa, Y. Sumino, T. Nanke, S. Ohya, N. Sonoda, T. Hirao, *J. Am. Chem. Soc.* **1997**, *119*, 2745–2746; b) Y. Sumino, N. Harato, Y. Tomisaka, A. Ogawa, *Tetrahedron* **2003**, *59*, 10499–10508.
[10] a) G. A. Molander, C. N. Wolfe, *J. Org. Chem.* **1998**, *63*, 9031–9036; b) G. A. Molander, C. Alonso-Alija, *J. Org. Chem.* **1998**, *63*, 4366–4373.
[11] W. G. Skene, J. C. Scaiano, F. L. Cozens, *J. Org. Chem.* **1996**, *61*, 7918–7921.
[12] a) W. Kaiser, C. G. B. Garrett, D. L. Wood, *Phys. Rev.* **1961**, *123*, 766–776; b) D. L. Wood, W. Kaiser, *Phys. Rev.* **1962**, *126*, 2079–2088; c) J. D. Axe, P. P. Sorokin, *Phys. Rev.* **1963**, *130*, 945–952.
[13] E. Prasad, R. A. Flowers II, *J. Am. Chem. Soc.* **2002**, *124*, 6357–6361.
[14] a) D. P. Curran, M. J. Totleben, *J. Am. Chem. Soc.* **1992**, *114*, 6050–6058; b) D. P. Curran, T. L. Fevig, C. P. Jasperse, M. J. Totleben, *Synlett* **1992**, 943–961.
[15] A. Yanase, *J. Phys. Soc. Jpn.* **1977**, *42*, 1680–1686.
[16] S. A. Payne, L. L. Chase, W. F. Krupke, L. A. Boatner, *J. Chem. Phys.* **1988**, *11*, 6751–6756.
[17] P. Dorenbos, *J. Phys. Condens. Matter* **2003**, *15*, 575–594.
[18] D. S. McClure, Z. Kiss, *J. Chem. Phys.* **1963**, *39*, 3251–3257.
[19] The decrease in excited state lifetime of Sm^{II} with increasing temperature suggests the fact that the 4f5d states start to become thermally occupied. Excited state Sm^{II} can thus radiate via electric dipole transitions, where only magnetic dipole transitions are allowed between f–f energy levels due to symmetry related selection rules. See ref. [12b] for details.
[20] N. J. Turro, *Modern Molecular Photochemistry*, The Benjamin/Cummings Publishing, California, **1978**.
[21] W. J. Evans, T. S. Gummersheimer, J. W. Ziller, *J. Am. Chem. Soc.* **1995**, *117*, 8999–9002.
[22] B. W. Knettle, PhD Thesis, Texas Tech University (USA), **2004**.
[23] G. J. Kavarnos, *Fundamentals of Photoinduced Electron Transfer*, VCH, New York, **1993**.

[24] R. C. Weast, *CRC Handbook of Chemistry and Physics*, 63rd ed., CRC Press, Boca Raton, Florida, **1983**.

[25] D. D. M. Wayner, V. D. Parker, *Acc. Chem. Res.* **1993**, *26*, 287–294.

[26] a) A. J. Bard, H. Lund, *Encyclopedia of Electrochemistry of the Elements*, *Vol. XIV*, Marcel Dekker, New York, **1980**; b) A. J. Bard, H. Lund, *Encyclopedia of Electrochemistry of the Elements*, *Vol. XII*, Marcel Dekker, New York, **1978**.

[27] R. A. Marcus, *Annu. Rev. Phys. Chem.* **1964**, *15*, 155–196.

[28] M. Shabangi, M. L. Kuhlman, R. A. Flowers II, *Org. Lett.* **1999**, *1*, 2133–2135.

[29] a) E. Prasad, K. R. Gopidas, *J. Am. Chem. Soc.* **2000**, *122*, 3191–3196; b) J. M. Hale, *Reactions of Molecules at Electrodes* (Ed.: N. S. Hush), Wiley, New York, **1971**, Chapter 4.

[30] R. J. Enemaerke, T. Hertz, T. Skrydstrup, K. Daasbjerg, *Chem. Eur. J.* **2000**, *6*, 3747–3754.

[31] L. Eberson, *Acta Chem. Scand.* **1982**, *B36*, 533–543.

[32] G. R. Moore, R. J. P. Williams, *Coord. Chem. Rev.* **1976**, *18*, 125–197.

[33] J. J. Gajewski, *Hydrocarbon Thermal Isomerizations*, Academic Press, New York, **1981**.

[34] D. P. Curran, X. Gu, W. Zhang, P. Dowd, *Tetrahedron* **1997**, *53*, 9023–9042.

[35] J. B. Shotwell, J. M. Sealy, R. A. Flowers II, *J. Org. Chem.* **1999**, *64*, 5251–5255.

[36] a) H. Weingarten, J. P. Chupp, W. A. White, *J. Org. Chem.* **1967**, *32*, 3246–3249; b) S. Mignani, D. Mouysset, I. Le Roy, L. Stella, *Synth. React. Inorg. Met.-Org. Chem. Synthetic Commun.* **2000**, *30*, 3685–3691.

Received: November 17, 2004